Quantitative and Multiplexed MicroRNA Sensing in Living Cells Based on Peptide Nucleic Acid and Nano Graphene Oxide (PANGO)

Soo-Ryoon Ryoo,[†] Jieon Lee,[†] Jinah Yeo,[‡,§] Hee-Kyung Na,[⊥] Young-Kwan Kim,[†] Hongje Jang,[⊥] Jung Hyun Lee,[§] Sang Woo Han,[⊥] Younghoon Lee,[⊥] Vic Narry Kim,[‡,§] and Dal-Hee Min*[,†,‡]

[†]Department of Chemistry, Seoul National University, Seoul, 151-747, Republic of Korea, [‡]Center for RNA Research, Institute for Basic Science (IBS), Seoul, 151-747, Republic of Korea, [§]School of Biological Sciences, Seoul National University, Seoul 151-747, Republic of Korea, and [⊥]Department of Chemistry, Korea Advanced Institute of Science and Technology (KAIST), Daejeon, 305-701, Republic of Korea

ABSTRACT MicroRNA (miRNA) is an important small RNA which regulates diverse gene expression at the post-transcriptional level. miRNAs are considered as important biomarkers since abnormal expression of specific miRNAs is associated with many diseases including cancer and diabetes. Therefore, it is important to develop biosensors to quantitatively detect miRNA expression levels. Here, we develop a nanosized graphene oxide (NGO) based miRNA sensor, which allows quantitative monitoring of target miRNA expression levels in living cells. The strategy is based on tight binding of NGO with peptide nucleic acid (PNA) probes, resulting in fluorescence quenching of the dye that is conjugated to the PNA, and subsequent recovery of the fluorescence upon addition of target miRNA. PNA as a probe for miRNA sensing offers many advantages including high sequence specificity, high loading capacity on the NGO surface compared to DNA and resistance against nuclease-mediated degradation. The present miRNA sensor allowed the detection of specific target miRNAs with the detection limit as low as ~1 pM and the simultaneous monitoring of three different miRNAs in a living cell.

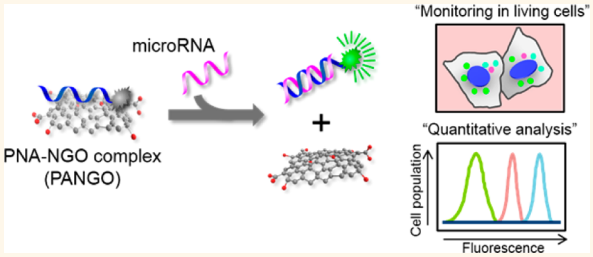

KEYWORDS: biosensor · graphene oxide · nanotechnology · peptide nucleic acid · RNA recognition

MicroRNAs (miRNAs) are a class of small-sized (~22 nucleotides), non-coding, single-stranded RNA molecules that play an important regulatory role in the expression of diverse genes by leading mRNA degradation or translational inhibition at the post-transcriptional level in a sequence-specific manner.[1−4] The dynamic changes of miRNA expression levels are associated with disease type and stage, responses to treatment and cellular status of differentiating stem cells.[5,6] Therefore, it is important to develop a sensing technology for quantitative measurement of the expression levels of specific miRNAs in order to practically utilize miRNA as useful biomarkers for diagnosis and prognosis in clinical processes and as a reliable indicator for cellular status.[4,7,8] Furthermore, a reliable miRNA sensing platform which enables monitoring of miRNA levels in living cells would be particularly attractive because of extended usefulness in basic biological research in addition to medical applications by providing a novel tool for studying miRNA related bioprocesses—for example, the discovery of new reagents which regulate miRNA expressions and the monitoring of miRNA dynamics during stem cell differentiation.

Among currently available common miRNA sensing techniques including Northern blot,[9] real-time quantitative PCR,[10] and microarrys,[11] none of them allow monitoring of miRNAs in living cells. Recently, nanomaterials such as graphene oxide (GO), oxidized form of graphene, have been utilized for the detection of miRNA *in vitro* as a fluorescence quencher of dye-labeled DNA probe or for the delivery of locked nucleic acid (LNA) integrated molecular beacon with help of cationic polymers.[12,13] Graphene is one-atom thick sheet of sp^2 carbon network arranged in perfect honeycomb

* Address correspondence to dalheemin@snu.ac.kr.

Received for review March 8, 2013 and accepted June 14, 2013.

Published online June 14, 2013
10.1021/nn401183s

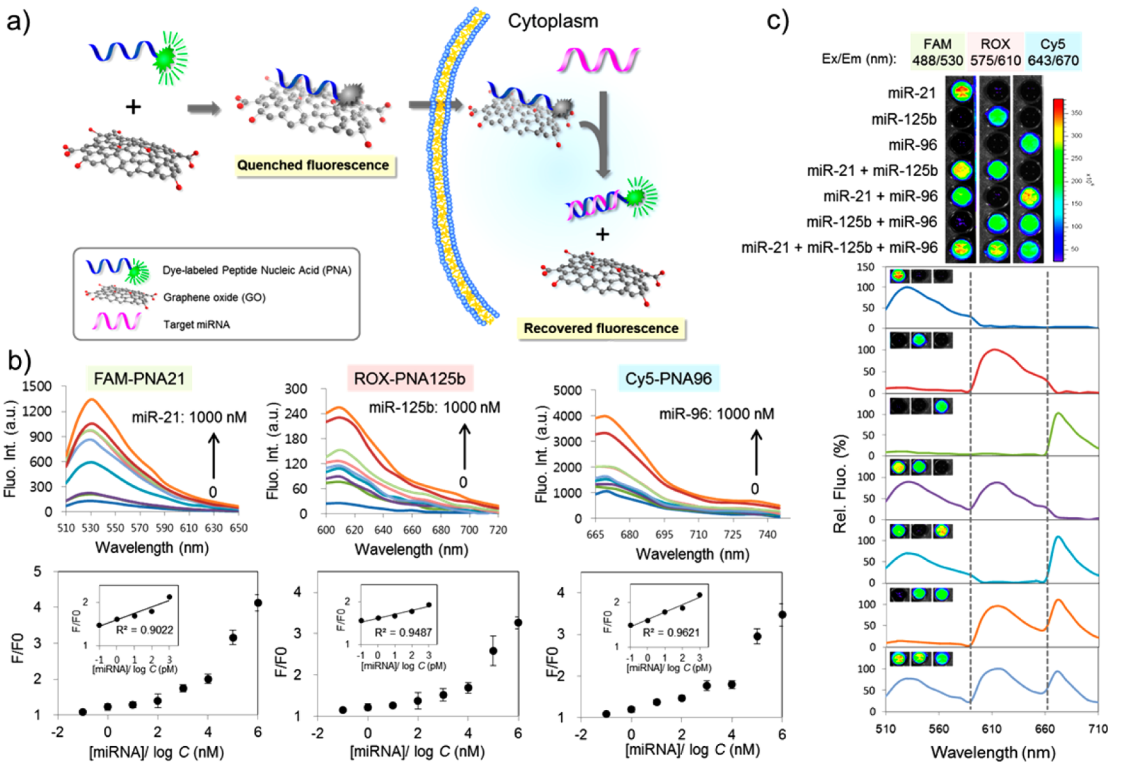

Figure 1. Scheme of strategy for a miRNA sensor based on NGO and PNA, and emission spectra and fluorescence images obtained for multiplexed miRNA sensing *in vitro*. (a) The fluorescence signal gets recovered when the fluorescent dye-labeled probes initially adsorbed onto the surface of NGO detach from NGO and hybridize with a target miRNA. (b) Three PNA probes—PNA21, PNA125b and PNA96—were designed for three different miRNA detection and prepared as conjugated with three different fluorescent dyes—FAM, ROX and Cy5. In each case, the quenched fluorescence was recovered upon addition of complementary miRNA in a concentration-dependent manner. Concentration of PNA was fixed as 100 pmol (in 60 μL) in all three cases. (F, Fluorescence intensity in the presence of miRNA; F0, Basal fluorescence intensity in the absence of miRNA.) (c) Simultaneous detection of multiple miRNAs *in vitro*. A mixture of three kinds of PNA (PNA21, PNA125b and PNA96)−NGO hybrid complexes were prepared in each well of a 96-well plate and individual well was treated with a mixed solution consisting of different combinations of three target miRNAs of which amount was 10 times higher than that of each PNA probe. Then, fluorescence intensities corresponding to FAM, ROX and Cy5 were measured and imaged. Fluorescent images and fluorescence emission spectra indicated that each PNA probe hybridized only with corresponding complementary miRNA in a sequence-specific manner, without notable cross-reactivity.

lattice and GO has been applied particularly for biosensors due to its high water dispersibility, affinity toward aromatic rings and hydrophobic biomolecules and fluorescence quenching capability. GO interacts with single-stranded oligonucleotides through $\pi-\pi$ stacking interaction with nucleobases and efficiently quenches fluorescence of dyes present nearby.[14−16] Although several GO-based approaches for miRNA detection have been developed,[12,18,19] quantitative monitoring of intracellular miRNAs in living cells still remains an important challenge.[17] For example, polyethyleneimine (PEI)-grafted graphene nanoribbon (GNR) has been developed to deliver LNA-integrated molecular beacon and thus, to detect intracellular miRNA.[12] In the study, positively charged PEI played a role as a material to load and deliver negatively charged LNA-beacon into cells. GNR was simply used as a nanocarrier for the delivery of PEI-LNA beacon. However, PEI is considered cytotoxic, and therefore, the combination of PEI and LNA is not ideal for intracellular sensors.

Here, we report a miRNA sensing platform composed of dye-labeled peptide nucleic acid (PNA) and nanosized GO (NGO) for simple, sensitive, quantitative, real-time monitoring of multiple miRNAs in living cells. The miRNA sensor is based on the recovery of the quenched fluorescence of dye-labeled PNA that was tightly bound to the surface of NGO, upon addition of target miRNA (Figure 1a). PNA is a non-natural nucleic acid analog in which the backbones are held together by uncharged amide bonds rather than the negatively charged-phosphodiester bonds as in DNA.[20−23] The miRNA sensing strategy utilizing PNA as a probe and NGO as a fluorescence quencher allows high selectivity and specificity toward target miRNA with very low background signal and low cytotoxicity due to (1) advantages of PNA itself such as better thermal stability of its duplex with DNA or RNA than their counterparts DNA:DNA or RNA:RNA, resistance to enzyme-mediated degradation and high target specificity,[24] (2) stable binding of neutral, uncharged PNA toward negatively charged NGO surface compared to other negatively charged nucleic acids such as DNA or LNA, which then minimizes nonspecific detachment of the PNA probe from NGO surface, and (3) efficient

intracellular delivery of the PNA–NGO complex without assistance of additional transfection reagent or highly positively charged toxic surface modifier such as polyethyleneimine (PEI).

RESULTS AND DISCUSSION

We first prepared GO sheets by using a modified Hummers' method previously reported.[25] NGO was then prepared with a final concentration of 1 mg/mL in distilled water after sonication of the aqueous GO solutions. We analyzed NGO by Raman, Fourier transform infrared (FT-IR), and UV–vis spectroscopy; zeta potential analysis; dynamic light scattering; atomic force microscopy; and elemental analysis (Supporting Information Figure S1 with detailed explanation in the legend). The zeta potential value of NGO was measured as about −17.9 mV with overall size of 0.05–300 nm and average thickness of about 1.03 nm. All the analysis data indicate the successful preparation of NGO.

Next, we evaluated the fluorescence quenching capability of the prepared NGO. We designed and prepared three different PNA probes conjugated with three different fluorescent dyes complementary for the selected three kinds of miRNAs expressed in cancer cell lines (probes: carboxy fluorescein (FAM)-PNA21, 6-carboxy-X-rhodamine (ROX)-PNA125b and cyanine 5 (Cy5)-PNA96; target miRNAs: miR-21, miR-125b and miR-96, sequences are shown in Supporting Information Figure S2). We then optimized the relative amounts of the dye-labeled PNA and NGO to give more than 99% quenching of the fluorescence by measuring fluorescence spectra of the dye-labeled PNA probes in the presence of varying amounts of NGO. The analysis revealed that the addition of 1 μg of NGO resulted in complete fluorescence quenching of 190 pmol of FAM–PNA21, 135 pmol of ROX–PNA125b and 200 pmol of Cy5–PNA96 within 10 min (Supporting Information Figure S3). This optimized ratio between the dye-PNA probes and NGO was used for the detection of miRNAs in the present study unless otherwise indicated. The resulting PNA–NGO complex is referred to as PANGO.

We next demonstrated the fluorescence recovery of the PANGO upon addition of chemically synthesized target miRNAs of various concentrations. The fluorescence signal was intensified as the concentration of added miRNA increased from 0 to 1000 nM (Figure 1b). The fluorescence intensity gradually increased within a range of 0–1000 nM of miRNA and the detection limit was estimated as low as ~1 pM (detection limit (DL) = 3.3 × (standard deviation/slope of the calibration curve)).

Next, we evaluated the sequence specificity and the multiplexed sensing capability of the miRNA sensor in homogeneous solution. A mixture of three kinds of PANGO complexes were prepared by using FAM–PNA21, ROX–PNA125b and Cy5–PNA96, and transferred in every well of a 96-well plate and each individual well was then treated with a different mixed solution consisting of different combinations of three target miRNAs. Fluorescent images and fluorescence emission spectra corresponding to FAM, ROX and Cy5 obtained from the multiwell plate indicated that PNA probes hybridized only with complementary miRNA in a sequence-specific manner and simultaneously sensed multiple miRNAs in a single homogeneous solution (Figure 1c). As a control, exposure of PANGO to miRNA with scrambled sequence gave no notable changes in fluorescence intensity (Supporting Information Figure S4). Collectively, our data suggest that the PANGO allows high-throughput monitoring of many samples containing multiple different miRNAs with low background and no notable cross-reactivity.

For the present strategy, PNA was chosen as a probe among other oligonucleotides due to its capability of tighter binding toward complementary miRNA than DNA. Also, PNA possesses neutral backbone unlike DNA or LNA exhibiting negatively charged phosphate backbones which may exert repulsive force to the negatively charged NGO at physiological pH. This kind of repulsion may facilitate nonspecific detachment of the probe from NGO surface and reduce quenching efficiency of NGO due to weakened interaction between the probe and NGO, which may exhibit high background signals in complex biological environment such as cell cytoplasm. In reality, to achieve ~100% fluorescence quenching, FAM–DNA required about four times higher amount of NGO than FAM–PNA (1.05 μg NGO for DNA and 0.3 μg NGO for PNA, DNA and PNA; 40 pmol, respectively) (Figure 2). To test robustness of the PNA–NGO interaction, FAM–PNA21–NGO and FAM–DNA21–NGO complexes were, respectively, treated with cell lysates prepared from the repeated freeze/thaw processes of HeLa cells which are expected to contain no intact complementary RNAs. We observed little changes in fluorescence intensity from FAM–PNA21–NGO complex upon addition of the cell lysates even after 1 h incubation (Figure 2a). However, fluorescence corresponding to FAM was highly intensified from the FAM–DNA21–NGO complex over time after treatment with cell lysates (about 1×10^4 cells per 1 μL cell lysate), which indicates that various biomolecules present in cell lysates can disrupt the interaction of NGO with DNA, but not that with PNA. Upon treatment of various concentrations of miR-21 miRNA spiked in the cell lysate, fluorescence intensity of FAM–PNA–NGO complex increased in a miR-21 concentration dependent manner (Figure 2b). The data indicate that PNA–NGO interaction is highly stable unlike DNA–NGO interaction in cell lysates, and therefore, the PANGO is well suited for sensing of complementary miRNAs in complex biological samples and living system.

We next examined whether PANGO can detect miRNAs in living cells. For this study, we chose three

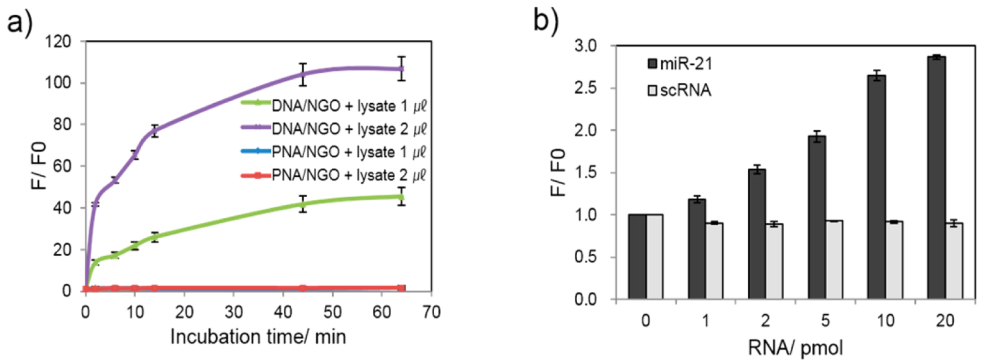

Figure 2. Stability and specificity test of PNA probe−NGO complex in HeLa cell lysate (a, the probe comparison: "DNA *vs* PNA"; b, specificity test of FAM−PNA21 against target miRNA (miR-21) and scrambled single-stranded RNA (5′-UGCGCUC-CUGGACGUAGCCUU-3′). (a) The FAM fluorescence signal of probe (DNA and PNA; 40 pmol, respectively) was quenched by the addition of NGO (1.05 μg NGO for DNA and 0.3 μg for PNA). After the prepared cell lysates (1×10^4 cells per 1 μL dispersed in buffer (20 mM Tris (pH 7.4) containing 100 mM NaCl, 5 mM KCl, 4.5 mM $MgCl_2$)) were incubated with the PNA or DNA probe−NGO complex solution, the fluorescence signals were monitored over time. In contrast to PNA−NGO, the notably high increase of fluorescence intensity was observed in the case of DNA−NGO in cell lysates. (b) Changes in the fluorescence of PNA probe were monitored in the cell lysates containing spiked-in RNAs (miR-21 or scRNA). The PNA probe recognized only complementary target RNA sequence, miR-21, and showed the increased fluorescence intensities in a concentration-dependent manner, whereas the addition of scRNA induced no increase of the fluorescence intensity.

different cancer cell lines—MCF-7 (early stage breast cancer cell), MDA-MB-231 (invasive human breast cancer cell line, late-stage cancer model) and MDA-MB-435 (melanoma cell line). The cells were cultured, incubated with FAM−PNA21−NGO complex for 14 h and then, fluorescent images of the cells were obtained after extensive washing. MiR-21 miRNA acts as an oncogene and antiapoptotic factor, which is up-regulated in many cancer cell lines.[26,28] Images of the cells showed that the intracellularly delivered FAM−PNA21−NGO induced the increase in fluorescence signal of FAM with different intensity in each cell line, suggesting different degrees of miR-21 miRNA expression levels in the three cancer cell lines (Figure 3a). The intensity of the fluorescence of the cells treated with FAM−PNA21−NGO was next quantified by flow cytometric analysis (Figure 3b). However, the FAM−scPNA−NGO (where scPNA stands for scrambled PNA having mismatched sequence) complex induced no changes in fluorescence of the cells, which indicates the fluorescence increase is sequence specific. Consistent with other reports,[29] MCF-7 and MDA-MB-231 exhibited higher expression of miR-21 than MDA-MB-435 and this relative miR-21 expression levels were also confirmed by the end point analysis of semi qRT-PCR (Figure 3c). As controls, when the cells were incubated with only FAM−PNA21, NGO alone or FAM-scPNA alone, fluorescence increase was not observed in the cells (Supporting Information Figure S5).

We next carried out MTT assay to evaluate cytotoxicity of NGO. Treatment of NGO induced little reduction in the viability of all the three cancer cells and HeLa cell by showing over 90% cell viability upon treatment of the NGO with concentrations up to 200 μg/mL (Supporting Information Figure S6). Throughout the present study for miRNA sensing, we used NGO of less than 12 μg/mL, which ensures ~100% viability of all the cells we tested.

To monitor dynamic changes in miRNA expression levels inside living cells, we used HeLa cells expressing miR-29a miRNA in a tetracycline-inducible manner.[30] The HeLa cells were first incubated with doxycycline (a tetracycline analog, 5 μg/mL) for different time period to induce different levels of miR-29a, treated with FAM−PNA29a (target: miR-29a, see Supporting Information Figure S2 for sequence)−NGO complex for 14 h, and analyzed by fluorescence microscopy (Figure 4a) and flow cytometry (Figure 4b). Northern blotting was also performed to determine absolute amounts of the expressed miR-29a miRNA at each time point (Figure 4c). The fluorescent images and flow cytometric analysis indicate that the fluorescence corresponding to FAM−PNA29a was intensified inside the cells as induction time for miR-29a miRNA expression by doxycycline increased and plateaued after 48 h. Control samples (FAM−scPNA−NGO, FAM−scPNA, FAM−PNA29, or NGO) only barely increased fluorescence intensities in the doxycycline-treated HeLa cells (Supporting Information Figure S7). To correlate fluorescence intensity from our PANGO with actual amount of induced miR-29a in the HeLa cells, mean fluorescence obtained from flow cytometric analysis of the FAM−PNA29a−NGO treated cells in Figure 4b was plotted *versus* absolute absolute amount of miR-29a miRNA per cell calculated from Northern blotting in Figure 4c. The fluorescence intensity increased as the amount of miR-29a miRNA increased from 38.46 to 91.17 nM per cell, with correlation coefficient, *R*-value of 0.9765 (Figure 4d). In addition, difference of ~11.4 nM (calculated from the difference between 60.49 and 71.88 nM in the plot), corresponding to ~139 copies

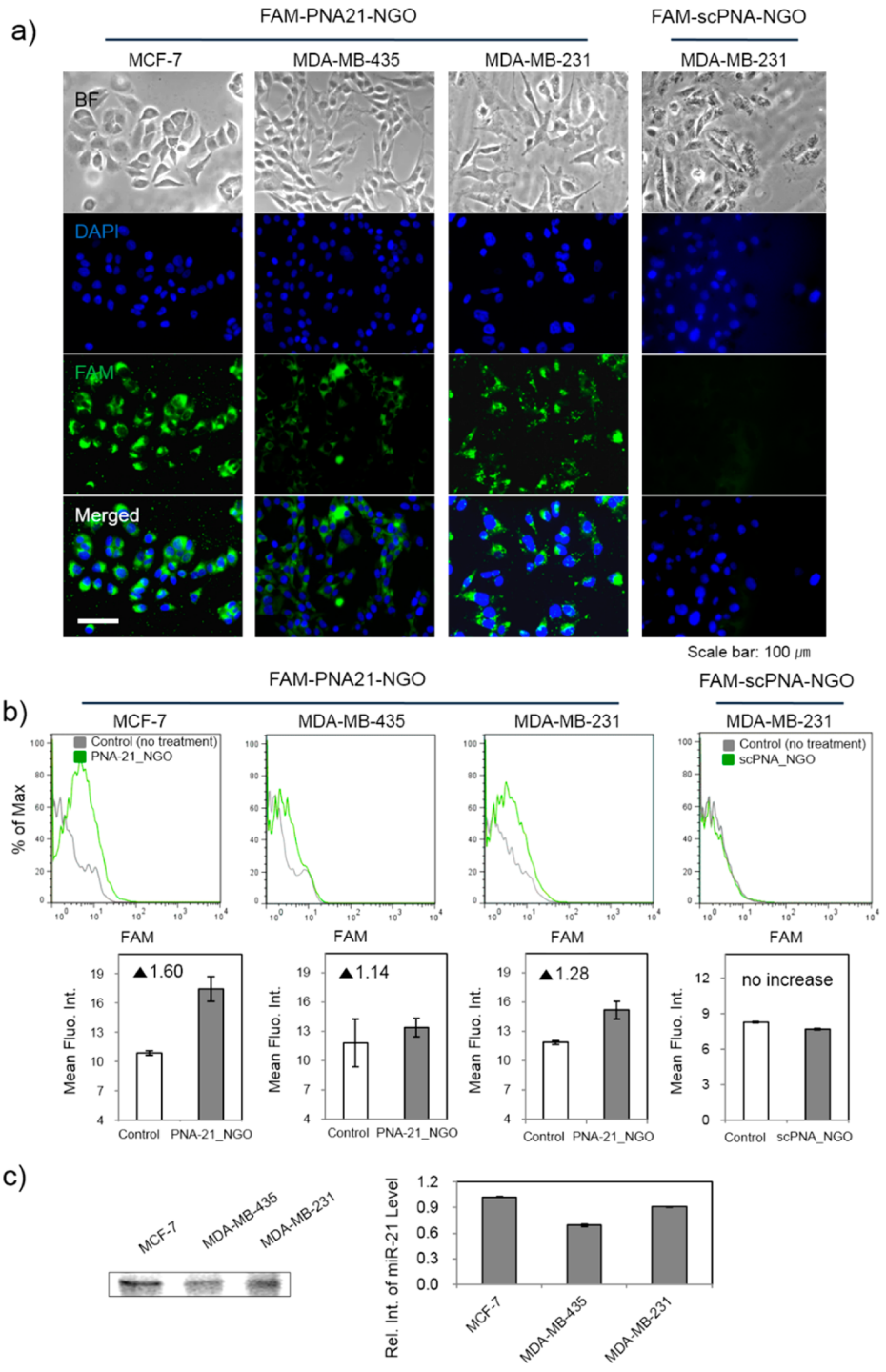

Figure 3. Qualitative and quantitative detection of miR-21 miRNA in three cancer cell lines—MCF-7, MDA-MB-435 and MDA-MB-231. (a) Fluorescent images of the cells were taken after 14 h of treatment of FAM−PNA21−NGO complex or FAM−scPNA−NGO complex to the cells, followed by extensive washing. The relative expression levels of miRNA could be qualitatively estimated from different degree of fluorescent intensities shown in the fluorescent images. As a control, treatment of FAM−scPNA, ROX−PNA125b or Cy5−PNA96 without NGO induced no fluorescent signal increase corresponding to FAM, ROX or Cy5 (Supporting Information Figure S5). (b) Quantitative measurement of miRNA-21 expression levels in the three cancer cell lines was performed using flow cytometry with the cells treated with FAM−PNA21−NGO complex. MCF-7 and MDA-MB-231 showed higher expression of miR-21 miRNA than MDA-MB-435 (p-value: 0.0219 for MCF-7, 0.4013 for MDA-MB-435, 0.0211 for MDA-MB-231 in the case of FAM−PNA21−NGO; p-value: 0.0643 for MDA-MB-231 in the case of FAM−scPNA−NGO). Confocal images are provided in Figures S10 and S11 in the Supporting Information. (c) As a comparison, semiquantitative end point PCR analysis was carried out to investigate miR-21 expression using the three cancer cell lines. Intensity of each band corresponding to miR-21 miRNA was measured and shown in a bar graph. Relative intensity of each band was normalized to U6 snRNA used as an internal control. The relative miR-21 expression level measured by the end point analysis of semi qRT-PCR was comparable to that obtained by the PANGO.

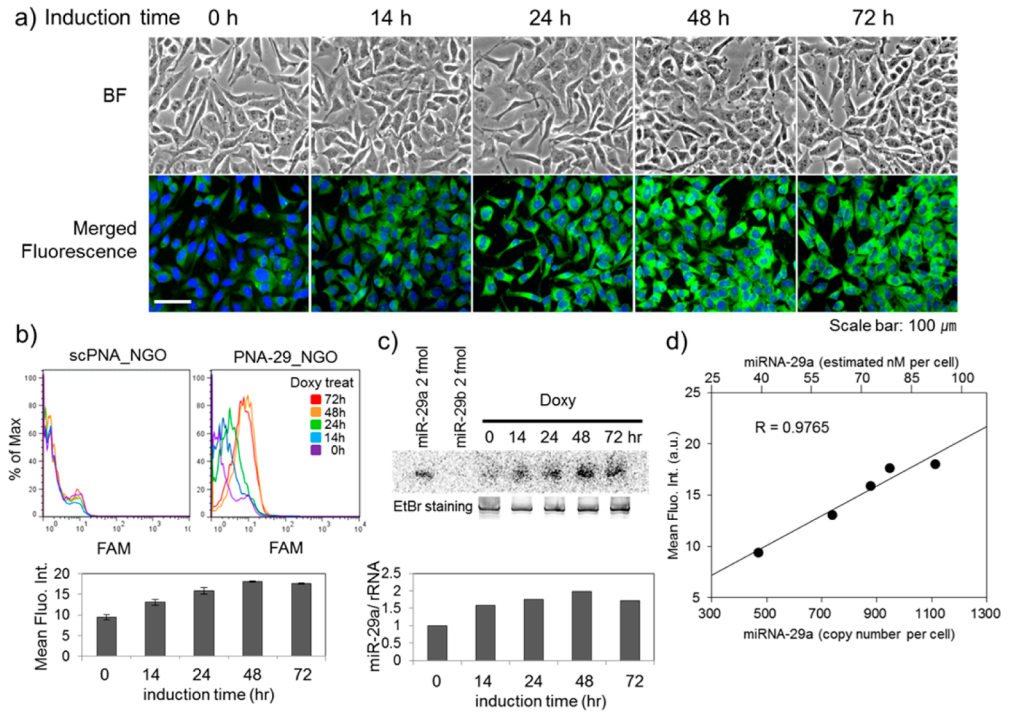

Figure 4. Monitoring of miR-29 miRNA in tetracycline-inducible miR-29a HeLa cell lines of which miR-29 miRNA expression increases upon treatment of tetracycline analog, doxycycline, in a time-dependent manner. (a) Gradually increasing fluorescence signals corresponding to FAM-labeled PNA-29a were visualized using a fluorescence microscope inside tetracycline-inducible miR-29a HeLa cells as induction time increased from 0 to 72 h. (b) Expression levels of miR-29a miRNA were quantified by flow cytometry and shown in a bar graph. (c) For comparison, Northern blotting was performed to measure miR-29a expression levels in the HeLa cells treated with doxycycline for different induction time. Synthetic miRNAs, miR-29a and miR-29b, were loaded as standards to estimate the intracellular levels of miR-29 in lanes 1 and 2. The results exhibited good correlation with the relative mean fluorescence intensities of flow cytometric analysis shown in panel b. (d) A plot of mean fluorescence intensities from flow cytometric analysis *versus* the intracellular levels of miR-29a miRNA estimated from Northern blot indicates that the present PANGO can quantitatively monitor miR-29 expression levels inside living cells (coefficient of correlation, R = 0.9765). The plot suggests that the PANGO can detect the differences in miRNA expression levels as little as ~11.4 nM in a living cell.

or ~0.5 fmol of miRNA in a single cell, could be easily discerned by using our PANGO. Although the gel-based (*e.g.*, Northern blotting) and the PCR methods (*e.g.*, real-time qRT-PCR) are widely used to characterize mature miRNA expression levels, RNA isolation step is still needed in these conventional methods. In contrast, our PANGO sensor allowed the quantitative monitoring of mature miRNA expression levels that increased over time in live cells by simple treatment of PNA–NGO complex to the cells without requiring any additional steps.

Often, multiple different miRNAs collaboratively regulate important cellular events at the same time, and thus, it is important to simultaneously monitor different miRNAs in cells. However, due to complex intracellular environment, it is not trivial to simultaneously detect the multiple miRNA in living cells, and therefore, none of the previously reported miRNA sensors demonstrated the multiplexed miRNA sensing in living cells. We now show that our PANGO realized the simultaneous detection of multiple target miRNAs in a living cell. MDA-MB-231 cells that were treated with a mixture of three PNA probes (FAM–PNA21, ROX–PNA125b and Cy5–PNA96) and NGO complex was analyzed by fluorescence microscopy and flow cytometry. MiR-21, miR-125b, and miR-96 miRNAs are previously reported to be expressed in MDA-MB-231 cells.[26,27] Fluorescent images showed three kinds of fluorescence signals in cells with different intensities and spatial distributions, and flow cytometry data revealed quantification of relative fluorescence intensities, which concurred well with Northern blotting analysis data by showing that miR-21 was the most abundant miRNA among the three miRNAs (Figure 5). However, in order to quantitatively measure relative miRNA expression levels, appropriate control experiments should be carefully designed because each fluorescent dye has different fluorescence quantum yield and, therefore, displays different fluorescence intensity even though the same amount of target miRNA is present. The results demonstrated that the multiple miRNA targets could be monitored in living cells by using PANGO. In addition, the present PANGO could be a new technology to reveal subcellular localization of various miRNAs in living cells, which is still largely unexplored research area due to lack of a convenient and practical technology.

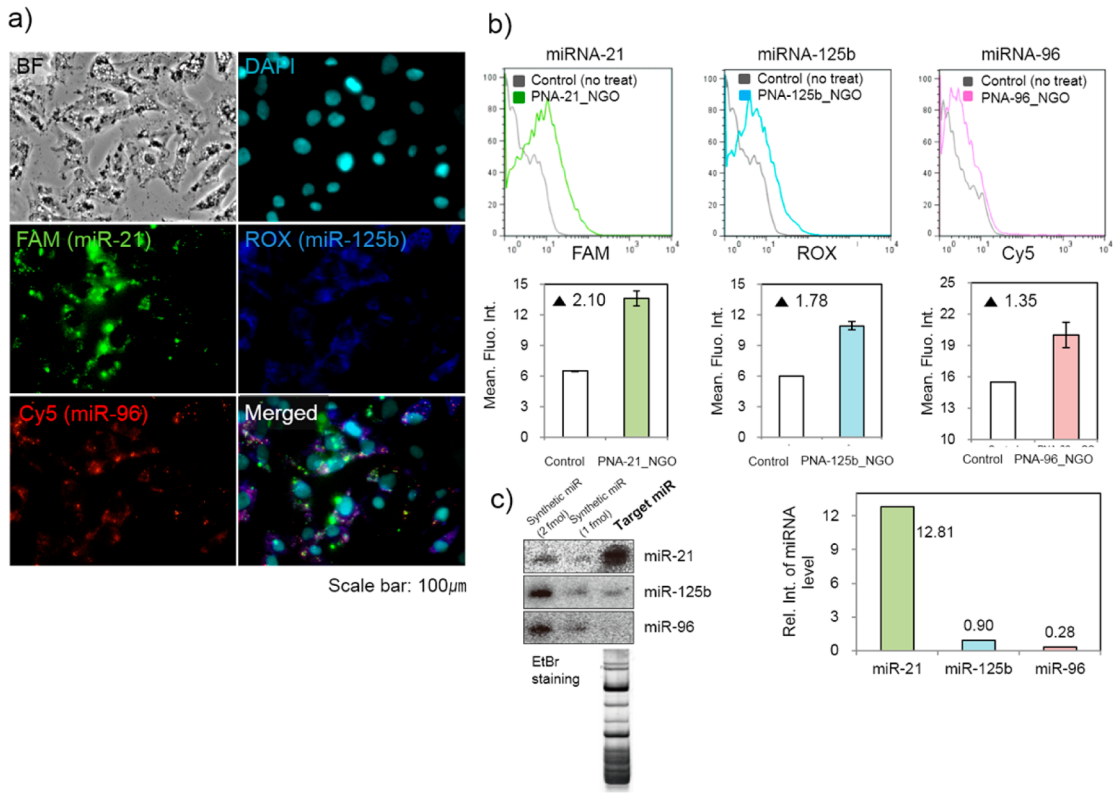

Figure 5. Simultaneous detection of three different miRNAs—miR-21, miR-125b and miR-96—in MDA-MB-231 cells. (a) A mixed solution of three PNA probes (FAM−PNA21, ROX−PNA125b and Cy5−PNA96)−NGO complex was treated with MDA-MB-231 for 14 h and then, fluorescent images were taken. Fluorescence corresponding to FAM−PNA21 was intense but fluorescence from ROX−PNA125b and Cy5−PNA96 was hardly observed in the fluorescent images, indicating that MDA-MB-231 cells abundantly express miR-21 but not miR-125b and miR-96 miRNAs. (b) The relative mean fluorescence of the MDA-MB-231 cells treated as in panel a was analyzed using a flow cytometer. (c) The expression levels of the three miRNAs were investigated using Northern blot analysis. Relative intensity of each band was normalized using synthetic miRNAs. The relative miRNA expression levels revealed by fluorescence imaging (a) and flow cytometric analysis (b) of the MDA-MB-231 cells treated with our PANGO were well correlated with those determined by Northern blotting analysis by showing that miR-21 was the most highly expressed miRNA among the three miRNAs.

CONCLUSIONS

We have demonstrated that the miRNA sensing strategy based on the PNA−NGO complex enabled quantitative monitoring of multiple miRNAs in homogeneous solutions and in living cells with high sequence specificity and low background signal. In addition, we further extended our strategy for the quantitative detection of miRNA expression levels that changed over time in living cells with high precision and discrimination power. The PANGO was robust enough to minimize nonspecific fluorescence signal and, thus, gave sensitive and quantifiable response to target miRNAs with low basal fluorescence even in living cells. We showed that PNA is superior to DNA as a miRNA sensing probe in the present PANGO by allowing tighter binding of the probe to NGO and, thus, exhibiting much lower background signals in complex biological sample such as cell lysate. We expect that the present miRNA sensing platform will be readily applicable for various miRNA related investigations, for example, the discovery of small molecules which regulate certain miRNA expression levels through high-throughput chemical screening in living cells, the detection of miRNAs as biomarkers in diseased tissues and even *in vivo*, and monitoring of dynamic changes in expression levels of specific miRNAs in stem cell differentiation.

MATERIALS AND METHODS

Materials. Natural graphite (FP 99.95%) was purchased from Graphit Kropfmühl AG (Hauzenberg, Germany). Sulfuric acid (H_2SO_4) was purchased from Samchun chemical (Seoul, Korea). Sodium nitrate ($NaNO_3$), hydrogen peroxide (30% in water) (H_2O_2), sodium chloride (NaCl), and magnesium chloride ($MgCl_2$) were purchased from Junsei (Japan). Potassium permanganate ($KMnO_4$) and G418 were purchased from Sigma-Aldrich (St. Louis, MO). Tris (hydroxymethyl)aminomethane-hydrochloride (Tris-HCl) was purchased from Fisher (Saddle Brook, NJ). The nuclease-free water was purchased from Ambion (Austin, TX). The microRNAs used in the study (miR-21, -125b, and -96) were synthesized by Bioneer (Daejeon, Korea). All microRNA and PNA sequences are listed in Figure S2 (HPLC profiles and MS spectra for all the PNA derivatives are located in Figure S9). Each PNA was labeled with three different fluorescent dyes and obtained from Panagene, Inc. (Daejeon, Korea). The fluorescent dyes were

covalently linked to the N-terminus of each PNA *via* an O-linker (AEEA, 8-amino-3, 5-dioxo-octanoic acid). The Trizol, SuperScript II Reverse Transcriptase, and Certified FBS were obtained from Invitrogen (Carlsbad, CA). Hygromycin B and doxycycline were purchased from Clontech.

Preparation of Nanosized Graphene Oxide (NGO). Graphene oxide sheets were synthesized according to a modified Hummers' method.[25] The natural graphite flake (0.5 g), $NaNO_3$ (0.5 g), and H_2SO_4 (23 mL) were mixed under vigorous stirring in an ice bath followed by the slow and cautious addition of $KMnO_4$ (3 g). Then the mixture was transferred to 35 °C water bath and stirred for 1 h. The distilled water (40 mL) was added and the bath temperature was increased up to 90 °C. The reaction mixture was stirred for 30 min followed by the addition of 100 mL of distilled water. Next, dropwise addition of 30% H_2O_2 (3 mL) was carried out. The reaction mixture was filtered by Buchner funnel and washed with distilled water for at least four times. The filter cake was dried in a desiccator and redispersed into distilled water to a final concentration of 3 mg/mL. The resulting solution was sonicated for 90 min to give nanosized graphene oxide sheets (NGO). The NGO suspension was prepared with a final concentration of 1 mg/mL.

Characterization of NGO. Raman analysis of the NGO was conducted by LabRAM HR UV/vis/NIR (Horiba jobin Yvon, France) using an Ar ion CW laser (514.5 nm) as an excitation source focused through a BXFM confocal microscope with an objective lens (50×, numerical aperture = 0.50). FT-IR measurement of NGO powder was carried out with an EQUINOX55 (Bruker, Germany) by the KBr pellet method. The UV−vis spectra of NGO were obtained with a SpectraMax Plus384 UV−vis spectrophotometer (Molecular Devices). Zeta potential value was measured by Zetasizer Nano ZS (Malvern Instruments, U.K.). The atomic force microscopy image and profile of NGO sheets were taken with an XE-100 (Park system) using a backside gold coated silicon probe (M to N, Korea).

Cell Culture. MDA-MB-435 and MDA-MB-231 cells were cultured in Dulbecco's Modified Eagle's Medium (DMEM) containing 4.5 g/L D-glucose and supplemented with 10% FBS (fetal bovine serum), 100 units/mL penicillin and 100 μg/mL streptomycin at 37 °C at 5% CO_2. MCF-7 cells were maintained in the growth media supplemented with 10 μg/mL bovine insulin (Sigma, St. Louis, MO). The tetracycline-inducible miR-29b-1∼29a HeLa cell line was provided by Prof. V. Narry Kim (Seoul National University, South Korea).[23]

MicroRNA Detection Using PANGO platform: In Test Tubes and Cell Lysates. (1) Single target detection: NGO solution was prepared as 50 μg/mL in distilled water. Each fluorescent PNA probe (10 μM per probe) was mixed with the NGO in buffer (Tris-HCl, pH 7.5) for 10 min at room temperature. The quenched fluorescence signals were monitored after the formation of PNA probe−NGO complex. A total of 30 μL of hybrid nanocomplex solution was mixed with 30 μL of target microRNA having a complementary sequence in a 96-well black plate, followed by addition of various concentrations (0−1000 nM) of microRNA. Fluorescence measurements were carried out using a fluorometer SynergyMx (Biotek, U.K.).

(2) Multitarget detection: In multitarget detections, FAM-, ROX-, and Cy5-labeled probes were mixed with NGO and followed by the addition of the target microRNAs. All other conditions were same as those in the single target detection. Fluorescence measurements were carried out using a fluorometer SynergyMx (Biotek, U.K.). The fluorescent images of mixtures (Figure 1c and Figure S4b) were collected using a charge-coupled device (CCD) camera of IVIS imaging system (Xenogen, CA). The imaging condition was as follows: exposure time = 10 s, field of view = 5 × 5 cm, and f/stop = 1.

(3) Cell lysate preparation using freeze/thaw method: HeLa cell extracts were prepared by resuspending of the cells in cold hypotonic buffer (20 mM HEPES, pH 8.0, 2 mM $MgCl_2$, 0.2 mM EGTA, 10% glycerol, 1 mM dithiothreitol) with 3 times of rapid quick-freeze in liquid nitrogen/thaw at 37 °C water bath. After the lysates were added to 0.4 M NaCl, the cleared lysates were collected by centrifugation for 20 min at 12 000 rpm (or max.) at 4 °C and carefully transferred to a fresh tube and stored at −80 °C until use.

TABLE 1. PCR Primers for Amplification of the Mature MicroRNAs

gene name		primer sequence (5′ → 3′)
miR-21	RT primer	CTCAACTGGTGTCGTGGAGTCGGCAATTCAGTTGAGTCAACATC
	Forward primer	ACACTCCAGCTGGGTAGCTTATCAGACTGA
U6 RNA	RT primer	CTCAACTGGTGTCGTGGAGTCGGCAATTCAGTTGAGAAAAATAT
	Forward primer	ACACTCCAGCTGGGTCGTGAAGCGTTC
	Reverse primer	GTGTCGTGGAGTCGGCAATTC

MicroRNA Detection in Live Cells. (1) Quantitative analysis using flow cytometer: Three kinds of cancer cell lines (MCF-7, MDA-MB-435, and MDA-MB-231) were chosen for a single target microRNA detection study *in vitro*. For multiple targets detection, MDA-MB-231 cell was used. Cells were seeded on 24-well cell culture plate at 6×10^4 cells per well. The cells were grown in an incubator at 37 °C and 5% CO_2. In a single target detection experiment, FAM−PNA21−NGO complex was treated to three kinds of cancer cell lines in a serum-free condition for 14 h at 37 °C. In multiple target detection study, three kinds of PNA probes−NGO complex (FAM-, ROX-, and Cy5-PNA probe (target: miR-21, -125b, and -96)) mixtures were added to MDA-MB-231 cells in a serum-free condition. After the cells were harvested using trypsin-EDTA treatment and washed with PBS, the fluorescence intensity of "live" cells was measured with a flow cytofluorometer (Beckton Dickinson). The fluorescence signal of each PNA probe was quantitatively analyzed in real time.

To observe the expression of miR-29a miRNA, doxycycline as an inducer was treated to miR-29b-1∼29a expressing HeLa cells. The FAM−PNA29−NGO complex was treated to cells following doxycycline treatment at indicated time point and intervals. Fluorescence signals of FAM were monitored with a flow cytometer.

(2) Fluorescence signal observation using fluorescence microscope: The fluorescence images of cells treated with each PNA probe−NGO complex were collected using a Ti inverted fluorescence microscope equipped with a 20× objective (Olympus IX 71, Tokyo, Japan) and a CoolSNAPcf charge-coupled device (CCD) camera (Photometrics, Tucson, AZ) with Metamorph image analysis software (Molecular Devices, Sunnyvale, CA).

Semiquantitative End Point PCR Analysis for the Determination of MicroRNA Expression Level. Total RNA was extracted by using Trizol reagent (Invitrogen) according to the manufacturer's instruction. Total RNA was quantified and the quality of total RNA was analyzed based on the 28S:18S rRNA ratio by using agarose gel electrophoresis. Total RNA samples (2 mg each) were used for reverse transcription under standard conditions (SuperScript II reverse transcriptase; Invitrogen) using a stem-loop gene-specific reverse transcription primer which was adapted from Varkonyi-Gasic *et al.*[31] The resulting cDNA was used as template in subsequent PCR amplifications. Primer sequences and PCR condition are listed in Table 1. The subsequent PCR reaction was performed as follows: (5 min at 95 °C, [30 s at 95 °C, 30 s at 55 °C, 30 s at 72 °C] × 30 cycles, 10 min at 72 °C. It should be noted that microRNAs expressed at lower levels required 35 cycles of PCR amplification to observe products. PCR products were separated on a 15% nondenaturing acrylamide gel and analyzed using a Gel Doc system (Bio-Rad, Hercules, CA). Relative intensity of each band normalized to U6 snRNA as an internal control was quantified using NIH ImageJ software.

RNA Measurement and Northern Blotting of miRNA. Cancer cells (MCF-7, MDA-MB-231, MDA-MB-435) and miR-29b-1∼29a HeLa were used for Northern blot analysis. The tetracycline-inducible miR-29b-1∼29a HeLa cell line was established by transfecting pcDNA-miR-29b-1∼29a plasmid and clonal selection of stably transfected cells. The doxycycline (tetracycline analog, 5 μg/mL) was treated for designated duration to induce miR-29.

TABLE 2. Sequences of the Northern Blot Probes and Synthetic miRNAs

oligonulceotides		sequence (5′ → 3′)
has-miR-125b probe	Northern probes	5′-TCACAAGTTAGGGTCTCAGGGA-3′
has-miR-96 probe		5′-AGCAAAAATGTGCTAGTGCCAAA-3′
has-miR-21 probe		5′-TCAACATCAGTCTGATAAGCTA-3′
has-miR-29a probe		5′- TAACCGATTTCAGATGGTGCTA-3′
has-miR-125b	synthetic miRNAs	5′-UCCCUGAGACCCUAACUUGUGA-3′
has-miR-96		5′-UUUGGCACUAGCACAUUUUUGCU-3′
has-miR-21		5′-UAGCUUAUCAGACUGAUGUUGA-3′
has-miR-29a		5′-UAGCACCAUCUGAAAUCGGUUA-3′

Total RNA was isolated with TRIzol reagent (Life Technologies). To measure the amount of miRNA by Northern blotting, 15−25 μg of RNA was resolved with 15% urea-polyacrylamide gel and transferred to Zeta-probe GT membrane (Biorad). Oligonucleotides complementary to each miRNA were 5′-end-labeled with [γ-^{32}P] ATP using T4 poly nucleotide kinase (T4 PNK) (Takara) and used as probes for hybridization to the membrane. An imaging plate (Fujifilm) was used to expose the radioactivity in the membrane, and the BAS-2500 imaging plate reader (Fujifilm) was used to measure the signal on the plate. Multi Gauge software (Fujifilm) was used for quantitation. The same membrane was reprobed for detection of different miRNAs. To determine the amount of synthetic miRNA used for normalization, a synthetic single strand RNA was labeled at the 5′-end with [γ -^{32}P] ATP using T4 PNK and resolved with 15% urea-polyacrylamide gel. The same method in Northern blotting was used to measure the radioactive signal in the gel. Northern probes and synthetic miRNAs are listed in Table 2.

Cytotoxicity Assay of NGO. Cancer cells (MCF-7, MDA-MB-231, MDA-MB-435) and miR-29b-1∼29a HeLa cell were seeded at 10 000 cells per well of a 96-well cell culture microplate. The MTT (3-(4,5-dimethylthiazol-2-yl)-2,5-diphenyltetrazolium bromide) assay was used to quantify the cell viability. Cells were incubated with NGO (at concentrations ranging from 0−200 μg/mL) and incubated for 14 h at 37 °C. Following NGO treatment, cells were rinsed with 1× PBS briefly and incubated with 20 μL of MTT stock solution (5 mg/mL) in each well to detect metabolically active cells. The cells were incubated for 2−3 h until the purple color developed. The media were discarded, and DMSO (200 μL) was added to each well to make insoluble formazan salt soluble. Then, the optical densities were measured at 560 nm and background absorbance at 670 nm (a reference wavelength) was subtracted.

Conflict of Interest: The authors declare no competing financial interest.

Acknowledgment. This work was supported by Basic Science Research Program (2011-0020322, 2011-0017356, 2008-0061892) and by the Research Center Program (EM1202) of Institute for Basic Science (IBS) through the National Research Foundation of Korea (NRF) funded by the Korean government (MEST).

Supporting Information Available: A description of the materials used, the detailed experimental procedures, and the analytical data. This material is available free of charge *via* the Internet at http://pubs.acs.org.

REFERENCES AND NOTES

1. Novina, C. D.; Sharp, P. A. The RNAi Revolution. *Nature* **2004**, *430*, 161–164.
2. He, L.; Hannon, G. J. Micrornas: Small RNAs with a Big Role in Gene Regulation. *Nat. Rev. Genet.* **2004**, *5*, 522–531.
3. Bartel, D. P. MicroRNAs: Genomics, Biogenesis, Mechanism, and Function. *Cell* **2004**, *116*, 281–297.
4. Kosaka, N.; Iguchi, H.; Ochiya, T. Circulating MicroRNA in Body Fluid: A New Potential Biomarker for Cancer Diagnosis and Prognosis. *Cancer Sci.* **2010**, *101*, 2087–2092.
5. Sun, W.; Julie Li, Y. S.; Huang, H. D.; Shyy, J. Y.; Chien, S. MicroRNA: A Master Regulator of Cellular Processes for Bioengineering Systems. *Annu. Rev. Biomed. Eng.* **2010**, *12*, 1–27.
6. Erson, A. E.; Petty, E. M. MicroRNAs in Development and Disease. *Clin. Genet.* **2008**, *74*, 296–306.
7. Calin, G. A.; Croce, C. M. MicroRNA Signatures in Human Cancers. *Nat. Rev. Cancer* **2006**, *6*, 857–866.
8. Pritchard, C. C.; Cheng, H. H.; Tewari, M. MicroRNA Profiling: Approaches and Considerations. *Nat. Rev. Genet.* **2012**, *13*, 358–369.
9. Kim, S. W.; Li, Z.; Moore, P. S.; Monaghan, A. P.; Chang, Y.; Nichols, M.; John, B. A Sensitive Non-Radioactive Northern Blot Method to Detect Small RNAs. *Nucleic Acids Res.* **2010**, *38*, e98.
10. Chen, C.; Ridzon, D. A.; Broomer, A. J.; Zhou, Z.; Lee, D. H.; Nguyen, J. T.; Barbisin, M.; Xu, N. L.; Mahuvakar, V. R.; Andersen, M. R.; *et al.* Real-Time Quantification of MicroRNAs by Stem-Loop RT-PCR. *Nucleic Acids Res.* **2005**, *33*, e179.
11. Yin, J. Q.; Zhao, R. C.; Morris, K. V. Profiling MicroRNA Expression with Microarrays. *Trends Biotechnol.* **2008**, *26*, 70–76.
12. Dong, H.; Ding, L.; Yan, F.; Ji, H.; Ju, H. The Use of Polyethylenimine-Grafted Graphene Nanoribbon for Cellular Delivery of Locked Nucleic Acid Modified Molecular Beacon for Recognition of MicroRNA. *Biomaterials* **2011**, *32*, 3875–3882.
13. De Smedt, S. C.; Demeesterm, J.; Hennink, W. E. Cationic Polymer Based Gene Delivery Systems. *Pharm. Res.* **2000**, *17*, 113–126.
14. Lu, C. H.; Yang, H. H.; Zhu, C. L.; Chen, X.; Chen, G. N. A Graphene Platform for Sensing Biomolecules. *Angew. Chem., Int. Ed.* **2009**, *48*, 4785–4787.
15. He, S.; Song, B.; Li, D.; Zhu, C.; Qi, W.; Wen, Y.; Wang, L.; Song, S.; Fang, H.; Fan, C. A Graphene Nanoprobe for Rapid, Sensitive, and Multicolor Fluorescent DNA Analysis. *Adv. Funct. Mater.* **2010**, *20*, 453–459.
16. Chou, S. S.; De, M.; Luo, J.; Rotello, V. M.; Huang, J.; Dravid, V. P. Nanoscale Graphene Oxide (nGO) as Artificial Receptors: Implications for Biomolecular Interactions and Sensing. *J. Am. Chem. Soc.* **2012**, *134*, 16725–16733.
17. Wang, Y.; Li, Z.; Hu, D.; Lin, C. T.; Li, J.; Lin, Y. Aptamer/Graphene Oxide Nanocomplex for *in Situ* Molecular Probing in Living Cells. *J. Am. Chem. Soc.* **2010**, *132*, 9274–9276.
18. Dong, H.; Zhang, J.; Ju, H.; Lu, H.; Wang, S.; Jin, S.; Hao, K.; Du, H.; Zhang, X. Highly Sensitive Multiple MicroRNA Detection Based on Fluorescence Quenching of Graphene Oxide and Isothermal Strand-Displacement Polymerase Reaction. *Anal. Chem.* **2012**, *84*, 4587–4593.
19. Cui, L.; Lin, X.; Lin, N.; Song, Y.; Zhu, Z.; Chen, X.; Yang, C. J. Graphene Oxide-Protected DNA Probes for Multiplex MicroRNA Analysis in Complex Biological Samples Based on a Cyclic Enzymatic Amplification Method. *Chem. Commun.* **2012**, *48*, 194–196.
20. Egholm, M.; Buchardt, O.; Nielsen, P. E.; Berg, R. H. Peptide Nucleic Acids (PNA). Oligonucleotide Analogues with an Achiral Peptide Backbone. *J. Am. Chem. Soc.* **1992**, *114*, 1895–1897.
21. Gaylord, B. S.; Massie, M. R.; Feinstein, S. C.; Bazan, G. C. SNP Detection using Peptide Nucleic Acid Probes and Conjugated Polymers: Applications in Neurodegenerative Disease Identification. *Proc. Natl. Acad. Sci. U.S.A.* **2005**, *102*, 34–39.
22. Yildiz, U. H.; Alagappan, P.; Liedberg, B. Naked Eye Detection of Lung Cancer Associated MiRNA by Paper Based Biosensing Platform. *Anal. Chem.* **2013**, *85*, 820–824.
23. Lu, Z.; Zhang, L.; Deng, Y.; Li, S.; He, N. Graphene Oxide for Rapid MicroRNA Detection. *Nanoscale* **2012**, *4*, 5840–5842.
24. Egholm, M.; Buchardt, O.; Christensen, L.; Behrens, C.; Freier, S. M.; Driver, D. A.; Berg, R. H.; Kim, S. K.; Norden, B.; Nielsen, P. E. PNA Hybridizes to Complementary Oligonucleotides Obeying the Watson-Crick Hydrogen Bonding Rules. *Nature* **1993**, *365*, 566–568.

25. Hummers, W. S.; Offeman, R. E. Preparation of Graphitic Oxide. *J. Am. Chem. Soc.* **1958**, *80*, 1339.
26. Iorio, M. V.; Ferracin, M.; Liu, C. G.; Veronese, A.; Spizzo, R.; Sabbioni, S.; Magri, E.; Pedriali, M.; Fabbri, M.; Campiglio, M.; *et al.* MicroRNA Gene Expression Deregulation in Human Breast Cancer. *Cancer Res.* **2005**, *65*, 7065–7070.
27. Terao, M.; Fratelli, M.; Kurosaki, M.; Zanetti, A.; Guarnaccia, V.; Paroni, G.; Tsykin, A.; Lupi, M.; Gianni, M.; Goodall, G. J.; *et al.* Induction of MiR-21 by Retinoic Acid in Estrogen Receptor-Positive Breast Carcinoma Cells: Biological Correlates and Molecular Targets. *J. Biol. Chem.* **2011**, *286*, 4027–4042.
28. Chan, J. A.; Krichevsky, A. M.; Kosik, K. S. MicroRNA-21 is an Antiapoptotic Factor in Human Gioblastoma Cells. *Cancer Res.* **2005**, *65*, 6029–6033.
29. Yan, L. X.; Wu, Q. N.; Zhang, Y.; Li, Y. Y.; Liao, D. Z.; Hou, J. H.; Fu, J.; Zeng, M. S.; Yun, J. P.; Wu, Q. L.; *et al.* Knockdown of MiR-21 in Human Breast Cancer Cell Lines Inhibits Proliferation, *in Vitro* Migration and *in Vivo* Tumor Growth. *Breast Cancer Res.* **2011**, *13*, R2.
30. Park, S. Y.; Lee, J. H.; Ha, M.; Nam, J. W.; Kim, V. N. MiR-29 MiRNAs Activate p53 by Targeting p85 Alpha and CDC42. *Nat. Struct. Mol. Biol.* **2009**, *16*, 23–29.
31. Varkonyi-Gasic, E.; Wu, R.; Wood, M.; Walton, E. F. Protocol: A Highly Sensitive RT-PCR Method for Detection and Quantification of MicroRNAs. *Plant Methods* **2007**, *3*, 12.